

RSC Advances



This is an *Accepted Manuscript*, which has been through the Royal Society of Chemistry peer review process and has been accepted for publication.

Accepted Manuscripts are published online shortly after acceptance, before technical editing, formatting and proof reading. Using this free service, authors can make their results available to the community, in citable form, before we publish the edited article. This *Accepted Manuscript* will be replaced by the edited, formatted and paginated article as soon as this is available.

You can find more information about *Accepted Manuscripts* in the [Information for Authors](#).

Please note that technical editing may introduce minor changes to the text and/or graphics, which may alter content. The journal's standard [Terms & Conditions](#) and the [Ethical guidelines](#) still apply. In no event shall the Royal Society of Chemistry be held responsible for any errors or omissions in this *Accepted Manuscript* or any consequences arising from the use of any information it contains.



Estradiol functionalized multi-walled carbon nanotubes as renovated strategy for efficient gene delivery

Sanyog Jain*, Kaushik Thanki, Nagesh Kumar Pandi and Varun Kushwah

Received 00th January 20xx,
Accepted 00th January 20xx

DOI: 10.1039/x0xx00000x

www.rsc.org/

The present work focuses on the development and characterization of the estradiol functionalized CNTs for efficient gene delivery applications. Simple carbodiimide chemistry was employed to synthesize Es-PEG-CNTs and the resulting conjugate authenticated by various spectrometric and chromatographic techniques. The nanoplexes of the resulting conjugate were carefully optimized for maximum encapsulation of pDNA (for induction of GFP). The successful encapsulation of the pDNA within nanoplexes was assessed using agarose gel electrophoresis and DNase protection assay. Exhaustive cell culture experiments have been conducted to evaluate the potential of nanoplexes in inducing the GFP expression in estrogen positive and estrogen negative cell lines. The results revealed 19.33-fold and 3.29-fold higher in vitro transfection in estrogen positive MCF-7 cells as compared to that of plain pDNA and Lipofectamine®, respectively. The remarkably higher transfection could be attributed to the intracellular localization of the surface functionalized nanoplexes in the vicinity of nucleus with pearson's coefficient >0.9. Interestingly, >80% cell viability was noted for Es-PEG-CNTs in contrast to that of non functionalized CNTs and lipofectamine which were found to be relatively toxic at tested concentrations. The potential of the developed nanocarrier was also challenged by intratumoral injection in animals and similar results were also noted in in-vivo experiments. To conclude, the developed nanoplexes pose great potential in delivering the pDNA for difficult to treat diseases such as cancer.

Introduction

Recent advances in the field of drug delivery systems have paved the way for efficient gene therapy which would have been nightmare otherwise. Gene therapy has proved itself as a reliable and realistic way out to address the difficult to treat diseases such as cancer, chronic obstructive pulmonary disease, diabetes, etc. The success of gene therapy could be attributed to its ability to deliver cargo at targeted site of action. A series of nanocarriers such as liposomes, polymeric nanoparticles, liquid crystalline nanoparticle, etc. have been explored till date for both temporal and spatial targeting thereby avoiding untoward effects. Further, a variety of homing targeting ligands have also been employed till date for achieving efficient gene delivery. In our previous reports, we have explored the potential of hyaluronic acid-polyethyleneamine complexes¹⁻³ and polyelectrolyte coated lipoplexes⁴ as novel transfecting agents.

Surface functionalized carbon nanotubes have recently gained

focus as a versatile and promising delivery carrier for variety of diseases⁵. The principle driving forces for surface functionalization are the inherent problems associated with pristine CNTs such as extremely low solubility in both aqueous and organic vehicles, higher chances of aggregation, cytotoxicity, low circulation half-life and lack of surface properties^{6,7}. Furthermore, it has been widely accepted that functionalization of CNTs improves their delivery behaviour such as high aspect ratio, tailored made surface chemistry, better payload capabilities, favourable biodistribution and so on⁸. Mechanistic insights on drug loading within CNTs suggest the formation of pi-pi stacking interactions, for most of the cases, by aligning the drug molecules within the hollow carbon layers⁹. Utilizing the same hypothesis, various scientists including authors' group have exhaustively explored surface functionalized CNTs for efficient cancer therapy⁸⁻¹⁰. However, an alternative mechanism has also been proposed for interaction of CNTs with nucleic acids such as pDNA wherein the latter forms helical structures over CNTs¹¹. Furthermore, higher nuclear targeting could be achieved by functionalization of nanocarriers with homing ligands such as estradiol. Estrogen receptors (ERs), in particular ER- α is preferentially located on both plasma membrane and nuclear membranes. The stimulation of these receptors by estradiol leads to both genomic and nongenomic signalling.^{12,13} Further conjugation of estradiol to pharmaceutical carriers results into both cellular and intracellular, organelle specific targeting for efficient management of disease conditions wherein the ERs are

Centre for Pharmaceutical Nanotechnology, Department of Pharmaceutics,
National Institute of Pharmaceutical Education and Research (NIPER), Sector 67,
Phase X, SAS Nagar (Mohali), Punjab - 160062, India

* Corresponding author: Dr Sanyog Jain

Email: sanyogjain@niper.ac.in, sanyogjain@rediffmail.com

Tel: +91172-2292055, Fax: +91172-2214692

Electronic Supplementary Information (ESI) available: [details of any supplementary information available should be included here]. See DOI: 10.1039/x0xx00000x

overexpressed, such as cancer.¹⁰ The authors' group previously explored the potential of estradiol functionalization over CNTs to demonstrate higher antitumor efficacy of doxorubicin by employing the intranuclear targeting capabilities of homing ligands¹⁰. On similar line of action, the intracellular localization of docetaxel in the vicinity of the nucleus was achieved upon loading into estradiol functionalized PLGA nanoparticles¹⁴.

In the present work, the authors' aim to explore the potential of surface functionalized CNTs as renovated carriers for gene delivery and assesses various aspects ranging from rationalized vector design, physicochemical evaluation, stability studies, mechanistic cell culture experiments and in vivo studies. The vector design comprised of estradiol as targeting ligand, PEG spacer and multiwalled carbon nanotube backbone while polylysine has been employed as stabilizer and payload enhancer.

Materials and Methods

Materials

Pristine (p) MWCNTs (purity >95%, length 1–5 μm , and diameter 20–30 nm) were procured from Nanovatech Pvt. Ltd., U.S. Sulphuric acid, nitric acid (69–72%), disodium hydrogen phosphate, sodium acetate, sodium bicarbonate, thionyl chloride, sodium lauryl sulfate, copper sulfate, and thiobarbituric acid were purchased from Loba Chemie Pvt. Ltd., India. Poly-L-lysine, minimum essential medium (MEM), fetal bovine serum (FBS), antibioticantimycotic solution, PEG bisamine (Mw =3500) and methoxy-PEG were procured from JenKem Technology. 17 β -Estradiol (E2), succinic anhydride, dicyclohexyl carbodiimide (DCC), N-hydroxysuccinimide (NHS), 2, 2'-(ethylene dioxy) bis-(ethylene amine) EDDBE, Carbonyldiimidazole (CDI), Tris, bromophenol blue (BPB), ethidium bromide (EtBr), sodium dodecyl sulfate (SDS), Triton X-100, ethylene diamine tetra acetic acid (EDTA), xylene cyanol (XC), neutral red (NR), rhodamine 123 (Rh123), 4',6-diamidino-2-phenylindole dihydrochloride (DAPI), rhodamine B isothiocyanate (RITC), 3-(4,5-dimethylthiazol-2-yl)-2,5-diphenyltetrazolium (MTT), and 7,12-dimethylbenz [α] anthracene (DMBA \geq 95% pure) were purchased from Sigma-Aldrich Chemical Co. (St. Louis, MO, USA). DNase I was purchased from Fermentas Molecular Biology Tools. The plasmid purification kit and Superfect was purchased from Qiagen (France) while Lipofectamine 2000 was purchased from Invitrogen. All kits for biochemical estimations were procured from Accurex, Biomedical Ltd., Mumbai. Deionized (Milli-Q) and Millipore filtered (pore diameter 0.22 μm) water was used throughout the experiments. Tissue culture plates were procured from Nunc, Roskilde, Denmark. All other chemicals and reagents were of analytical grade and procured from local suppliers.

Extraction of plasmid DNA

Plasmid DNA (pDNA) encoded for enhanced green fluorescence protein was extracted from competent *Escherichia coli* (DH5 α) vectored previously using pEGFP-N₃ gene procured from Addgene, USA. Plasmid purification kit

and maxiprep columns (Qiagen) were employed for isolation of pDNA from *E. coli* exhibiting resistance to Kanamycin treatment following manufacturer's protocol. The purity of the obtained pDNA was confirmed by assessing the absorbance ratio (260/280 nm) and agarose gel electrophoresis.⁴

Synthesis and characterization of functionalized multiwalled carbon nanotubes (MWCNTs)

Surface oxidation of pristine MWCNTs, initial length 1-5 μm , was achieved using acid treatment (20 mg/ml, H₂SO₄ and HNO₃ in ratio 3:1) followed by bath sonication for 5 min and reflux at 80° C for 8 h¹⁵. The oxidized CNTs (Ox-MWCNTs) thus obtained were washed extensively and purified using deionized water, and air dried. In separate set of experiments, process variables such as oxidation time were optimized for achieving efficient oxidation (**Supplementary information**)¹⁶. The surface oxidation was measured as a function of dynamic light scattering, zeta potential and scanning electron microscopy (SEM, Hitachi, S-3400N, Japan).

The functionalization of Ox-MWCNTs with PEG-Estradiol was attained in three steps comprising of (i) synthesis of estradiol 17- β -hemisuccinate (Es-hemisuccinate), (ii) PEGylation of Es-hemisuccinate and finally (iii) conjugation of carboxyl terminals of Ox-MWCNTs to the amino groups of synthesized Es-hemisuccinate resulting into formation of estradiol functionalized MWCNTs with PEG-3500 as spacer (Es-PEG-MWCNTs) (Figure 1). A detailed synthesis protocol is previously reported by our group and exactly same was followed with slight modifications as per laboratory conditions¹⁰. The chemical structure of the synthesized conjugates was authenticated using routine spectroscopic and chromatographic tools. Simultaneously, employing standard protocol, PEGylation of the Ox-MWCNTs was also carried out to synthesize PEG-MWCNTs for comparison purposes¹⁷.

Preparation of pDNA loaded functionalized MWCNTs nanoplexes

Nanoplexes were prepared by incubating functionalized MWCNTs (Ox-MWCNTs, PEG-MWCNTs, E₂-PEG-MWCNTs) with pDNA for 12 h at room temperature in presence of auxiliary component poly-L lysine (10 $\mu\text{g}/\text{ml}$). Theoretical loading of pDNA in all cases was kept as 1 $\mu\text{g}/\text{ml}$ ¹.

Evaluation of the prepared nanoplexes

Physicochemical characterization

The prepared nanoplexes were evaluated for particle size and zeta potential using dynamic light scattering (DLS, Nano ZS, Malvern Instruments, UK). The particle size was average of 5 measurements while zeta potential was estimated taking average of 20 measurements. The entrapment efficiency of the nanoplexes was determined using standard Picogreen assay[®] (Promega, USA) with heparin as displacing agent¹⁸.

Morphological analysis

The shape and surface morphology of the developed nanoplexes was studied using transmission electron microscopy, (TEM, Philips, Japan). Briefly, 400-mesh carbon coated grids were loaded with samples and allowed to air dry. Specimens were viewed under the microscope at an accelerating voltage of 100-200.0 kV.

The Δ absorbance_{260 nm} was monitored spectrophotometrically at the interval of 5 min. The results were further confirmed by gel electrophoresis. Briefly, the DNase I in the above samples was inactivated using 5 μ l, 100 mM EDTA and resulting mixture was incubated with 10 μ l, 5 mg/ml heparin

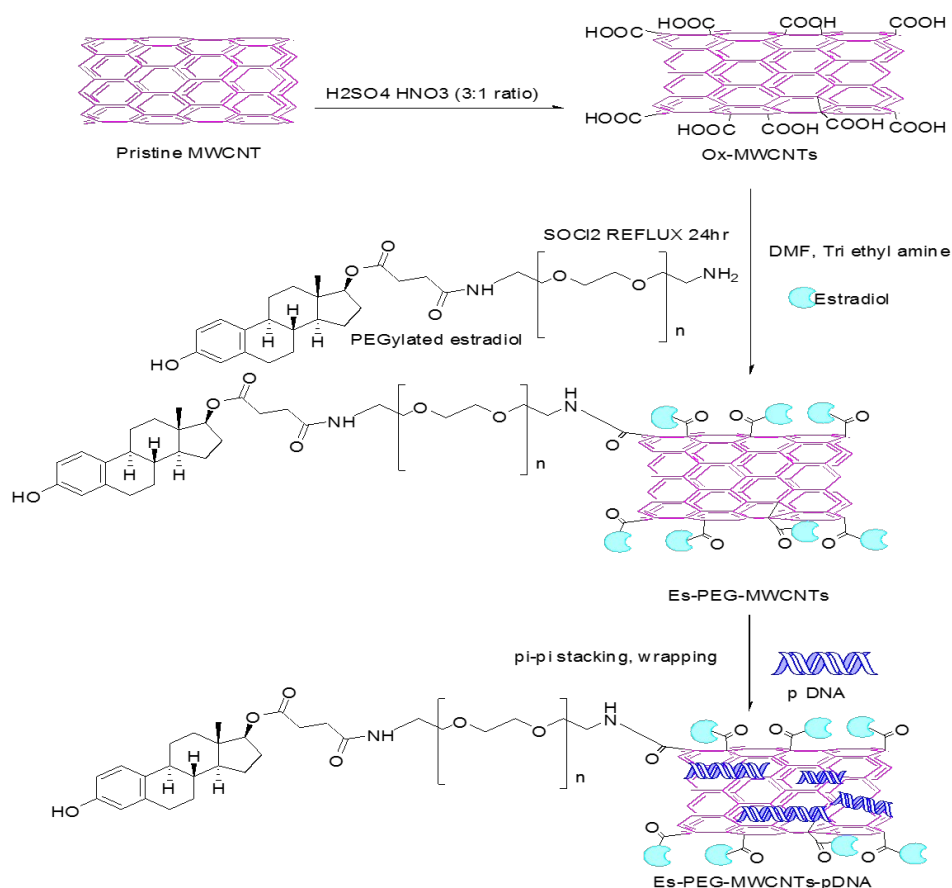


Figure 1: Schematic representation for functionalization of MWCNTs

Agarose gel electrophoresis

The prepared nanoplexes were added to the loading buffer comprising of a tracking dye, xylene cyanol and charged to individual wells containing 0.8% agarose gel and electrophoresed at 100 V for 45 min in TAE buffer (40 mM Tris-HCl, 1% (v/v) acetic acid, 1 mM EDTA). Subsequently, ethidium bromide (EtBr) stained gels were visualized using UV trans illuminator to assess the bands of corresponding pDNA².

DNase protection assay

Standard DNase protection assay was performed to assess the potential of developed nanoplexes in shielding the loaded pDNA against nucleases. Briefly, naked pDNA and prepared nanoplexes were incubated with 10 μ l DNase I (1000 units/ml) contained in buffer solution comprising of 10×10^{-3} M Tris-Cl, 150×10^{-3} M NaCl and 1×10^{-3} M $MgCl_2$, pH 7.4 for 30 min at 37°C for 30 min. Further, 50 μ l, 50×10^{-3} M Mg^{2+} solution was also added to the resulting mixture for initiating the reaction.

for 2 h to dissociate the complexes. Subsequently, the entire mixture was electrophoresed in 0.8% agarose to assess pDNA replaced from the complex.

Serum stability

The clinical utility of the developed nanoplexes was assessed as a function of stability in presence of serum. Briefly, developed nanoplexes equivalent to 10 μ g of pDNA were incubated with equal volume of phosphate buffer saline containing 50% v/v fetal bovine serum (Sigma, USA) for 4 h at 37°C. The incubated nanoplexes were then monitored for any changes in physicochemical parameters such as particle size, polydispersity index and zeta potential. Separately, the replaced pDNA, if any, was assessed using ethidium bromide intercalation assay¹.

Cell culture experiments

Cell culture

Human breast adenocarcinoma cells (MCF-7) and human cervix adenocarcinoma cells (HeLa) were grown in Minimum

Essential Medium Eagle (MEM, Sigma) supplemented with sodium bicarbonate (2.2% w/v), sodium pyruvate (10 mM), 10% fetal bovine serum (FBS, Sigma, USA) and antibiotic-antimycotic solution (Sigma, USA) at 37°C under 5% CO₂ environment. The cell culture medium was changed at every alternate day till 90% confluency was achieved. Once confluent, cells were trypsinized with 0.25% trypsin-EDTA solution (Sigma, USA) and utilized for further studies.

In vitro transfection

MCF-7 and HeLa cells were seeded at cell density of 10⁵ cells/well in 6 well plates and allowed to adhere overnight. Subsequently, the culture medium was aspirated and supplemented with fresh media and incubated with formulated nanoplexes (plain pDNA, Ox-MWCNTs, PEG-MWCNTs and Es-PEG-MWCNTs), equivalent to 1 µg/well pDNA for 4 h at 37°C. Post incubation, the cell culture medium containing nanoplexes was aspirated and reincubated with fresh culture medium for additional 48 h. The culture medium was then aspirated and cells washed twice with phosphate buffer saline (PBS, pH 7.4) and visualized under confocal laser scanning electron microscope (CLSM, Olympus FV1000, Japan), using He-Ne green laser at excitation wavelength 489 nm and emission wavelength 510 nm) for expression of EGFP within cells, qualitatively. In separate set of experiments, the treated cells were lysed using triton X 100 and centrifuged to pellet out cellular debris. The supernatant was then subjected to quantitative estimation of EGFP using standard protocol. Briefly, 2 µl of supernatant was loaded on a Nanodrop spectrofluorimeter (NanoDrop 3300, Thermo Fisher Scientific, USA) to assess EGFP (excitation 488 nm and emission 509 nm). The observed values of fluorescence intensity were normalized per µg of protein against control cells (untreated), estimated separately using Bradford method. In separate set of experiments the in vitro transfection efficiency of the prepared nanoplexes was also assessed using flow cytometry following standard protocol¹.

Intracellular localization of nanoplexes

The intracellular localization of the developed nanoplexes loaded with coumarin-6 was also evaluated in estrogen positive MCF-7 cells. Briefly, MCF-7 cells were seeded at cell density of 10⁵ cells/well in 6-well culture plates and incubated with C-6 loaded nanoplexes for 4 h at 37°C. Post incubation, cells were washed twice with Hank's balanced buffer solution and cells were fixed using 2.5% v/v glutaraldehyde solution (Sigma, USA). The cells were then permeabilized with Triton X-100 and nuclei labeled with DAPI (10 ng/ml, 30 s). The labelled cells were then visualized under a CLSM (Olympus FV1000, USA) using green and blue channels. Operational parameters for instrument were kept constant for all the samples. Pearson's co-efficient for co-localization of green and blue fluorescence within the captured images was estimated using data processing software of CLSM.

Cell cytotoxicity

The cell cytotoxicity of the developed nanoplexes was evaluated on both MCF-7 cells and HeLa cells using standard MTT assay. Briefly, cells were seeded at density of 10⁴ cells/well in 96 well plates and allowed to adhere overnight. Cells were then exposed to various formulations (plain pDNA, Ox-MWCNTs, PEG-MWCNTs, Es-PEG-MWCNTs and Lipofectamine®) equivalent to 1 µg/well of pDNA for 4 h at 37°C. Subsequently, the culture medium containing treatment was aspirated and reincubated with fresh media for additional 48 h. Post incubation, the culture medium was aspirated and each well added with 150 µl of MTT solution (500 µg/ml in PBS). Formazan crystals were allowed to form for additional 3-4 h and excess solution was aspirated carefully. The generated MTT formazan were dissolved in 200 µl DMSO and absorbance measured spectrophotometer at 550 nm (ELISA plate reader, BioTek, USA). The cell viability was estimated using following formula:

$$\text{Cell viability} = \frac{A_{\text{test}} - A_{\text{blank}}}{A_{\text{control}} - A_{\text{blank}}} \times 100$$

Where, A_{test} , A_{blank} and A_{control} are absorbance of test, blank and control samples, respectively.

In vivo gene expression studies

Animal studies protocols were duly approved by the Institutional Animal Ethics Committee (IAEC), NIPER, India. All the animal studies were performed in accordance with guidelines of the Committee for the Purpose of Control and Supervision of Experiments on Animals (CPCSEA), India. Female Sprague Dawley rats (200-250 g) were procured from central animal facility, NIPER and used for in vivo gene expression studies following standard protocol already established in our laboratory. Briefly, animals were orally administered weekly with 7,12-Dimethylbenz(a)anthracene (DMBA) pre-dissolved in sunflower oil, 45 mg/kg for 3 consecutive weeks and subjected to standard housing for 10 weeks, *Ad libitum*^{1, 19}. Tumor bearing animals were randomly divided in the 6 groups each containing three animals and intratumoral injection of vehicle treated, plain pDNA, Ox-MWCNTs, PEG-MWCNTs, Es-PEG-MWCNTs and Lipofectamine®, equivalent to 1 µg of pDNA. After 48 h, the animals were sacrificed humanely and tumors dissected. Representative tumors from each group were visualized under photon imager (Biospace, France) for in vivo gene expression. Instrumental parameters were previously set by normalizing the autofluorescence emerging from tumors of control animals (untreated) and subsequent images were captured at that particular threshold value.

Statistical Analysis

All in vitro and in vivo data are expressed as mean ± standard deviation (SD) and mean ± standard error of mean (SEM), respectively. Statistical analysis was performed with Sigma Stat (Version 2.03) using one-way ANOVA followed by Tukey-

Kramer multiple comparison test. $P < 0.05$ was considered as statistically significant difference.

Results

Authentication of extracted pDNA

The purity of extracted pDNA was determined as a function of absorbance ratio at 260/280 nm using UV Spectrophotometer and was found to be 1.84 when resuspended in sterile Tris buffer (Supplementary information). Furthermore, the concentration of the extracted pDNA stock estimated by normalizing the turbidity was found to be 232.6 $\mu\text{g/ml}$. It was also found that extracted pDNA was free from any genomic DNA or RNA (Supplementary information).

Synthesis and characterization of functionalized MWCNTs

A series of functionalized MWCNTs (OX-MWCNTs, PEG-MWCNTs and Es-PEG-MWCNTs) were synthesized and extensively characterized using spectroscopic techniques (Supplementary information). Table 1 depicts various physicochemical properties of synthesized MWCNTs. Figure 2 reflects the representative SEM images of functionalized MWCNTs.

Table 1: Quality attributes of functionalized MWCNTs

Functionalized MWCNTs	Particle size (nm)	PDI	Zeta potential (mV)
Pristine MWCNTs	Aggregation	-	-
Ox-MWCNTs	351.2 \pm 23.2	0.659 \pm 0.14	-37.9 \pm 2.8
PEG-MWCNTs	231.8 \pm 15.7	0.394 \pm 0.13	-5.3 \pm 2.1
Es-PEG-MWCNTs	263.6 \pm 18.5	0.379 \pm 0.15	-2.4 \pm 3.3

Date expressed as Mean \pm SD (n=6)

Preparation and evaluation of functionalized MWCNTs based nanoplexes

Blank formulations were first prepared to identify the optimum concentration of nanoplexes by dispersing the synthesized MWCNTs conjugate and auxiliary components in sterile water (Table 2). As evident, it was found that nanoplexes with desired quality attributes were formed at concentration of 60 $\mu\text{g/ml}$ in all cases of Ox-MWCNTs, PEG-MWCNTs and Es-PEG-MWCNTs.

Physicochemical evaluation of pDNA loaded nanoplexes

pDNA loaded nanoplexes were then prepared by incubating various functionalized MWCNTs conjugates (60 $\mu\text{g/ml}$), poly-L-lysine (10 $\mu\text{g/ml}$) and pDNA (10 $\mu\text{g/ml}$) for 30 min at room temperature in sterile water. A linearly increasing trend in entrapment efficiency was noted from Ox-MWCNTs, PEG-MWCNTs and Es-PEG-MWCNTs (Table 3). The concentration of

poly-L-lysine and pDNA for preparing nanoplexes was optimized previously during preliminary studies (data not shown). Further, Figure 3 depicts the representative TEM images of the pDNA loaded various nanoplexes.

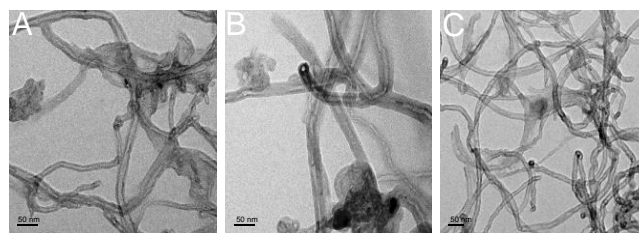


Figure 3: Representative TEM images of pDNA loaded (A) Ox-MWCNTs, (B) PEG-MWCNTs and (C) Es-PEG-MWCNTs

Agarose gel electrophoresis

The electrophoretic mobility of the complexed pDNA was completely retarded in all the cases of nanoplexes in contrast to that of plain pDNA whose mobility was maintained (Figure 4). The results are suggestive of sufficiently strong complexation thereby inhibiting the pDNA to mobilize against electric current.

DNase protection assay

Figure 5 depicts the changes in absorbance of various formulations incubated with DNase, emerging out of the degradation of DNA into its nucleotides. As evident, plain pDNA was completely degraded in presence of DNases within 20 min whereas no statistically significant difference in absorbance values was noted in case of nanoplexes indicative of superior DNase protection capabilities of developed nanoplexes. In separate set of experiments, the complexed pDNA was dissociated using heparin and replaced pDNA was quantified using EtBr intercalation assay which revealed no statistical significant difference ($p > 0.05$) in the entrapment efficiency of treated samples of nanoplexes while remarkable decrease in the fluorescence was noted for plain pDNA (data not shown). The results were further confirmed by Agarose gel electrophoresis.

Serum stability

Table 4 depicts the changes in various critical quality attributes of developed nanoplexes subjected to stability studies in presence of serum. As evident, no statistically significant ($p > 0.05$) changes in the critical quality attributes of the developed nanoplexes were observed suggesting their robustness nature against serum.

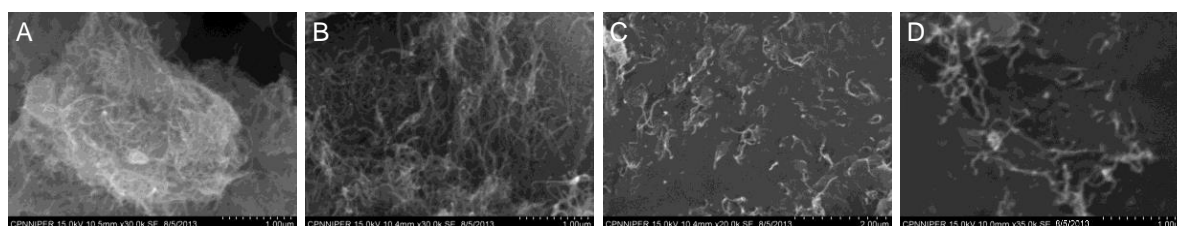


Figure 2: Representative SEM images of (A) pristine MWCNTs, (B) Ox-MWCNTs, (C) PEG-MWCNTs and (D) Es-PEG-MWCNTs

Table 2: Quality attributes of nanoplexes

Conc. (µg/ml)	Ox-MWCNTs		PEG-MWCNTs		Es-PEG-MWCNTs	
	Size (nm)	PDI	Size (nm)	PDI	Size (nm)	PDI
10	1159±10.7	1±0.016	560.6±9.5	0.245±0.426	803.7±5.8	0.618±0.069
20	1106±4.2	0.769±0.046	485.1±3.1	0.478±0.201	783.5±3.4	0.551±0.034
30	955.3±7.9	0.781±0.053	462.1±2.2	0.411±0.074	659.3±2.9	0.112±0.033
40	833.4±14.1	0.697±0.004	468.6±25.4	0.371±0.042	549.8±3.1	0.292±0.089
50	761.4±4.5	0.758±0.074	323.1±34.3	0.464±0.043	398.5±4.6	0.435±0.066
60	215.6±15.5	0.620 ±0.032	254.8±1.4	0.378±0.046	235.2±3.1	0.291±0.025
70	908.2 ±7.6	0.701±0.04	354.9±8.6	0.344±0.036	564.6±5.8	0.515±0.095
80	1105±2.4	0.930 ±0.105	447.9±9.5	0.371±0.029	566.3±4.8	0.378±0.068
90	1295±4.2	0.778±0.09	447.2 ±5.2	0.511±0.025	524.1±5.1	0.442±0.102
100	1422±3.9	1±0.98	523.3±6.8	0.504±0.066	443.5±4.2	0.368±0.099

Data expressed as Mean±SD (n=6)

Cell culture experiments

In vitro transfection

Figure 6 depicts the qualitative estimation of the in vitro transfection executed by developed nanoplexes against estrogen positive, MCF-7 cells and estrogen negative, HeLa cells. As evident, it was found that remarkably higher fluorescence of GFP was noted in case of developed nanoplexes and Lipofectamine® as compared to that of plain pDNA. The highest in vitro transfection was noted in case of Es-PEG-MWCNTs against MCF-7 cells as compared to all nanoplexes across both the cells lines with 19.33-fold and 3.29-fold higher transfection as compared to that of plain pDNA and Lipofectamine®, respectively (Figure 7). Interestingly, remarkable differences within the transfection efficiency of Es-PEG-MWCNTs were noted with MCF-7 and HeLa cells which could be attributed to the presence of estrogen receptor in former cells. The results were further confirmed using flow cytometric assessment of in vitro transfection studies revealing almost 78% of positive GFP positive population in case of Es-PEG MWCNTs as compared to ~45% in case of Lipofectamine® (Figure 8). Of note, no statistically significant differences were observed among all other formulation treatments for MCF-7 and HeLa cells however a slight increased mean values was observed in case of HeLa cells which could be attributed to relatively higher transfection capacity. To further confirm the contributory role of estradiol functionalization on the in vitro transfection efficiency, Es-PEG-MWCNTs was incubated with MCF-7 cells, previously exposed to higher concentration of estradiol. Interesting results were noted and in vitro transfection efficiency was found to be 12.18-fold and 2.04-fold higher as compared to that of plain pDNA and Lipofectamine®. Noteworthy, no statistical difference in the fluorescence of MCF-7 cells (Es saturated) and HeLa cells were observed when treated with Es-PEG-MWCNTs.

Table 3: Quality attributes of pDNA loaded nanoplexes

Nanoplexes	Particle Size (nm)	PDI	Zeta potential (mV)	Entrapment efficiency (%)
Ox-MWCNTs	231.8±14.2	0.621±0.030	+5.97±1.3	24.11±4.2
PEG-MWCNTs	286.4±7.8	0.382±0.049	+7.71±1.8	41.21±3.6
Es-PEG-MWCNTs	291.5±11.1	0.296±0.032	+6.92±0.9	83.45±3.5

Data expressed as Mean±SD (n=6)

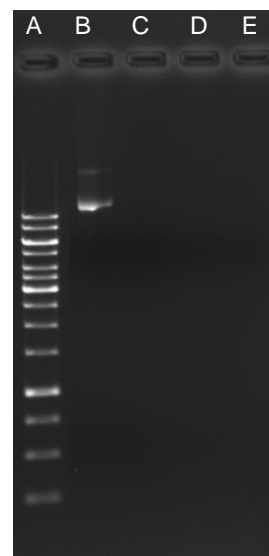


Figure 4: Gel retardation assay of (A) plain DNA, (B) Ox-MWCNTs, (C) PEG-MWCNTs and (D) Es-PEG-MWCNTs

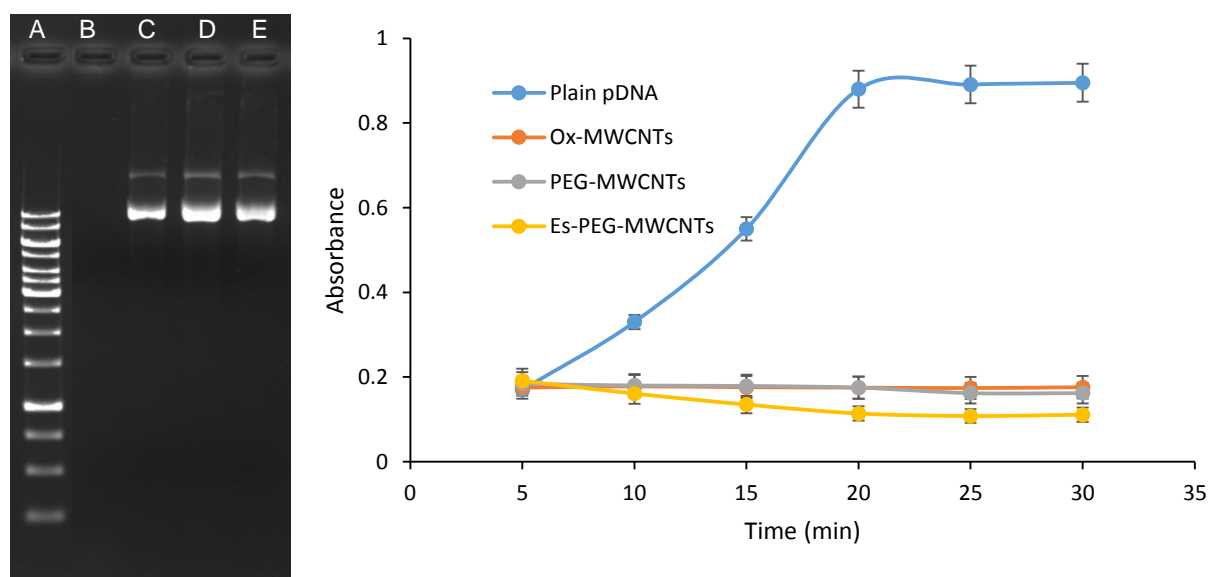


Figure 5: DNase protection assay for prepared nanoplexes: (I) Gel retardation assay of (A) plain DNA, (B) Ox-MWCNTs, (C) PEG-MWCNTs and (D) Es-PEG-MWCNTs (II) EtBr intercalation assay.

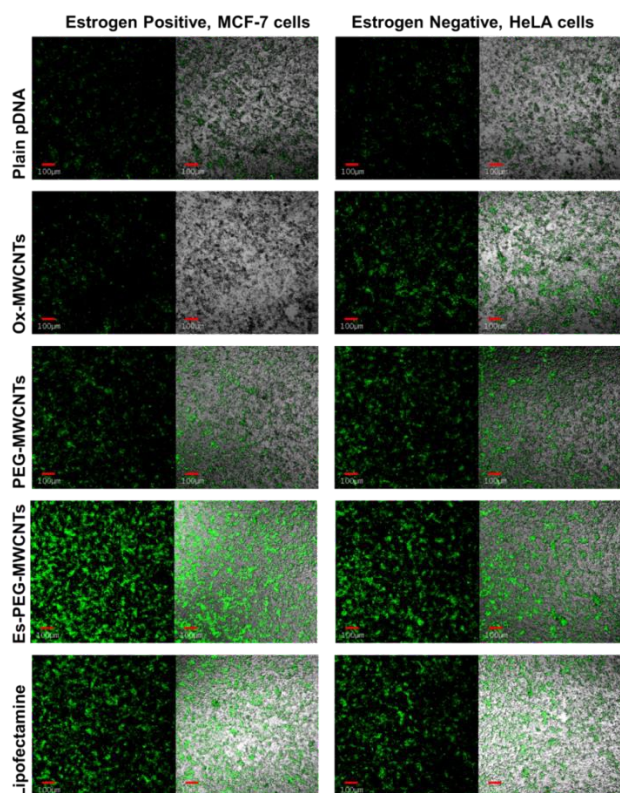


Figure 6: Representative CLSM images of cells transfected with pDNA loaded nanoplexes in MCF-7 and HeLa cells. Scale bar represents 100 μm.

Intracellular localization of prepared nanoplexes

The remarkably higher *in vitro* transfection was further confirmed by the intracellular colocalization studies wherein the Pearson's coefficient between coumarin-6 fluorescence representing Es-PEG-MWCNTs and blue fluorescence representing nucleus was found to be 0.929, which could be attributed to the estradiol functionalization. In contrast, the Pearson's co-efficient in case of non targeted nanoplexes was found to be 0.544 and 0.327 for PEG-MWCNTs and Ox-MWCNTs, respectively (Figure 9).

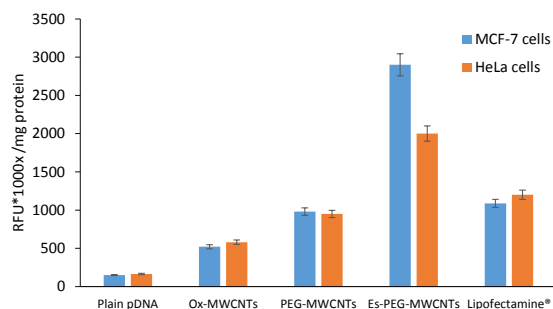


Figure 7: Quantitative estimation of *in vitro* transfection in MCF-7 and HeLa cells

Table 4: Serum stability studies for developed nanoplexes

Nanoplexes	Size (nm)		PDI		Zeta potential (mV)		Entrapment efficiency	
	Before	After	Before	After	Before	After	Before	After
Ox-MWCNTs	231.8±14.2	265.3±27.4	0.621±0.030	0.654±0.012	+5.97±1.3	-3.25±1.1	24.11±4.2	23.79±2.6
PEG-MWCNTs	286.4±7.8	320.5±38.3	0.382±0.049	0.391±0.056	+7.71±1.8	-2.47±0.3	41.21±3.6	40.02±3.1
Es-PEG-MWCNTs	291.5±11.1	312.6±25.2	0.296±0.032	0.301±0.036	+6.92±0.9	-2.29±0.2	83.45±3.5	81.41±3.5

Data expressed as Mean±SD (n=6)

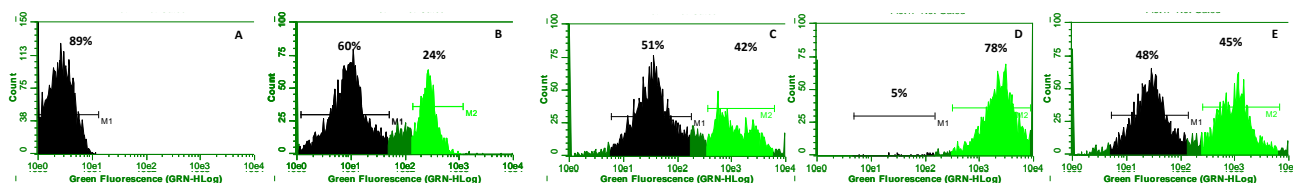


Figure 8: Flow cytometry based assessment of in vitro transfection efficiency in MCF-7 cell lines using (A) plain pDNA, (B) Ox-MWCNTs, (C) PEG-MWCNTs, (D) Es-PEG-MWCNTs and (E) Lipofectamine®

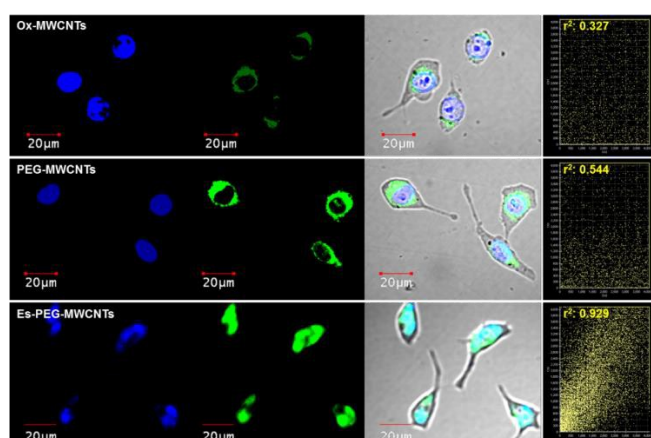


Figure 9: Intracellular localization of C-6 loaded nanoplexes. Channel 1, 2 and 4 depicts the blue fluorescence of DAPI, green fluorescence of coumarin-6 and overlay blue, green and differential image contrast (DIC), respectively. Channel 4 reflects the scattering plot for colocalization of blue and green fluorescence. Scale bar represents 20 μm.

Cell cytotoxicity studies

With remarkable transfection efficiencies, the obvious concern for cell cytotoxicity was also addressed using standard MTT assay and it was found that Es-PEG-MWCNTs showed marginal cell cytotoxicity (<10%) in both the cell lines. Interestingly, PEG-MWCNTs also exhibited lower cytotoxicity and values were <20% in both the cell lines (Figure 10). Notable cell cytotoxicity was seen in case of Ox-MWCNTs and Lipofectamine®.

In vivo gene expression

In vivo gene expression studies were further employed for assessing the performance of the developed nanoplexes in physiological conditions. Figure 11 depicts the fluorescence micrographs of tumors excised from animals treated with various pDNA loaded nanoplexes. The fluorescence emerging out of the tumors was attributed to that of EGFP produced by transfection of the tumor cells. Highest fluorescence was noted in case of Es-PEG-MWCNTs followed by PEG-MWCNTs,

Lipofectamine® and Ox-MWCNTs as compared to that of plain pDNA.

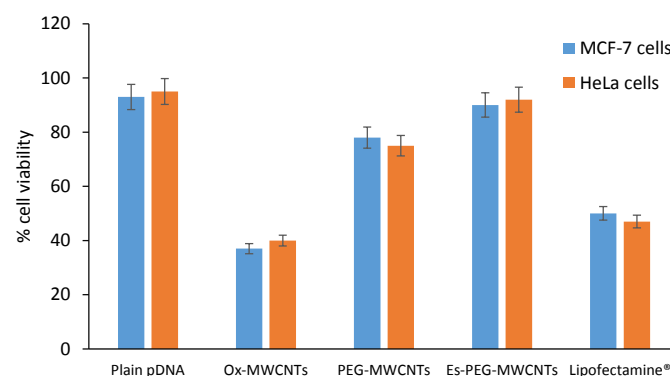


Figure 10: Cell toxicity of pDNA loaded nanoplexes in MCF-7 and HeLa cells

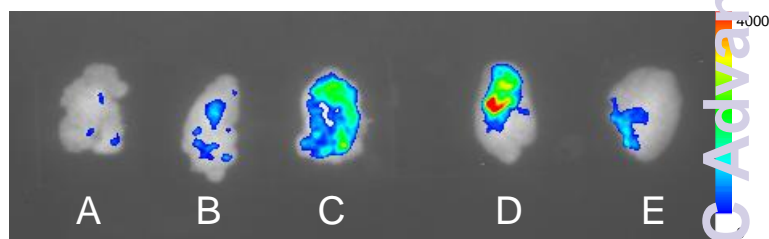


Figure 11: Images of the excised tumors showing GFP expression following intratumoral injection of (A) plain pDNA, (B) Ox-MWCNTs, (C) PEG-MWCNTs, (D) Es-PEG-MWCNTs and (E) Lipofectamine® in tumor bearing rats

Discussion

The present report focuses on the preparation and assessment of the surface functionalized carbon nanotubes with improved transfection efficiency thereby making them efficient carriers for nucleic acid delivery. Estradiol was employed as homing ligand for imparting targeting capabilities whereas poly-L-lysine was implemented to improve upon the loading of pDNA within carbon nanotubes^{10, 20}. Further, multiwalled carbon

nanotubes were used as backbone owing to relatively higher surface area and therefore higher number of functional groups for modifications and better biocompatibility as compared to single walled carbon nanotubes^{21,22}. As per standard protocol, oxidation of pristine CNTs was performed to yield surface active CNTs for subsequent functionalization (Table 1).¹⁶ In the present case, amine terminated Es-PEG derivative was covalently linked to carboxyl groups of oxidized MWCNTs and resulting conjugate extensively characterized. Further, formulation development and optimization studies revealed predominant role of solid content on formation of nanoplexes and subsequent critical quality attributes. (Table 2). Interestingly, it was important to note that once formed the nanoplexes were quite stable and retained the physicochemical properties even upon extreme dilutions revealing the stabilizing effects of poly lysine. As evident from Table 3, the entrapment efficiency of the nanoplexes increased as a function of functionalization revealing the allied mechanisms of self-assembling and molecular interactions, such as helical wrapping of pDNA over the walls of CNTs, apart from only charge based interactions.^{23,24} Careful optimization of the ratio of pDNA and CNTs revealed that self assembling properties were maximum observed at 60 µg/ml resulting into decrease in the particle size, even lower than that of plain CNTs (Table 1). Remarkably higher entrapment efficiency in case of Es-PEG-MWCNTs (i.e > 80%) further reveals the importance of hydrophobic end group modification in retaining the pDNA within the carrier by either interaction or preventing any possible leakage.

The integrity of the encapsulated pDNA was further established as a function of the agarose gel electrophoresis assay and DNase protection assay. Interestingly, the recovered pDNA from the nanoplexes upon heparin displacement was comparable to plain pDNA (data not shown). Subsequently, serum stability studies were performed which revealed the capability of the developed nanoplexes to retain the critical quality attributes even in presence of serum. The exhibited stability could be attributed to the relatively low surface charge of the developed nanoplexes (~5 mV) as compared to classically reported cationic vectors and relatively lower interaction of MWCNTs with cell culture media^{25,26}.

In vitro transfection efficiency studies revealed some interesting findings with the developed nanoplexes wherein differential transfection capabilities were noted for the developed formulation. The degree of transfection in different cell lines was observed as a function of the presence of estrogen receptor on the cell surface. The extent of transfection was higher in case of estrogen positive MCF-7 cells as compared to HeLa cells in which the estrogen receptors are relatively less expressed (Figure 6). The results were in line with our previous report⁴. The results were further corroborated using flow cytometry experiments (Figure 8). Interestingly, a gradual increase in the autofluorescence of GFP negative cell population was noted upon formulation treatment during flow cytometry experiments, which could be due to slight cellular distress upon uptake of nanoplexes. The remarkably higher

transfection efficiency was further corroborated using intranuclear colocalization of the Es-PEG-CNTs which was found to be >90% as compared to the 50% or less for non-targeted nanoplexes (Figure 9). Importantly, no observable cell cytotoxicity was seen in case of Es-PEG-CNTs in contrast to that of Lipofectamine® thereby revealing the great safety potential of the developed nanoplexes. The results of the in vitro transfection were further confirmed by in vivo transfection studies which also revealed relatively higher readout of green fluorescence, a measure of EGFP protein within tumor cells upon internalization of the plasmid DNA within nucleus (Figure 11).

Conclusions

The developed estradiol functionalized carbon nanotubes pose great potential for intracellular delivery of nucleic acids. The presented data corroborates the possibility of altering the intracellular fate of the nanocarriers with the help of homing devices such as estradiol. Although, the developed nanoplexes were not cytotoxic in cell culture but the in vivo toxicity studies could be further evaluated to further assess the safety potential of the developed system. Furthermore considering the very high serum stability, the developed nanoplexes opens new avenues for more therapeutically active targets and it could also be explored as step ahead towards clinical applications.

Acknowledgements

Authors are thankful to Indian National Academy of Sciences (INSA), Government of India for funding and Director, NIPER for providing necessary infrastructure facilities. KT and VK are also thankful to Council of Scientific and Industrial Research (CSIR) for financial assistance. Technical support by Mr. Rahul Mahajan is also duly acknowledged.

References

1. S. Jain, S. Kumar, A. Agrawal, K. Thanki and U. Banerjee, *RSC Advances*, 2015, **5**, 41144-41154.
2. A. Pathak, P. Kumar, K. Chuttani, S. Jain, A. K. Mishra, S. P. Vyas and K. C. Gupta, *ACS Nano*, 2009, **3**, 1493-1505.
3. A. Pathak, A. Swami, S. Patnaik, S. Jain, K. Chuttani, A. K. Mishra, S. P. Vyas, P. Kumar and K. C. Gupta, *J Biomed Nanotechnol*, 2009, **5**, 264-277.
4. S. Jain, S. Kumar, A. K. Agrawal, K. Thanki and U. C. Banerjee, *Mol Pharm*, 2013, **10**, 2416-2425.
5. V. S. Thakare, D. A. Prendergast, G. Pastorin and S. Jain, in *Targeted Drug Delivery: Concepts and Design*, Springer International Publishing, 2015, pp. 615-645.
6. R. Singh, D. Pantarotto, L. Lacerda, G. Pastorin, C. Klumpp, M. Prato, A. Bianco and K. Kostarelos, *Proc Natl Acad Sci U S A*, 2006, **103**, 3357-3362.
7. G. Pastorin, *Pharm Res*, 2009, **26**, 746-769.
8. M. Das, S. R. Datir, R. P. Singh and S. Jain, *Mol Pharm*, 2013, **10**, 2543-2557.

9. V. S. Thakare, M. Das, A. K. Jain, S. Patil and S. Jain, *Nanomedicine (Lond)*, 2010, **5**, 1277-1301.
10. M. Das, R. P. Singh, S. R. Datir and S. Jain, *Mol Pharm*, 2013, **10**, 3404-3416.
11. G. Dovbeshko, O. Repnytska, E. Obraztsova, Y. V. Shtogun and E. Andreev, *Semiconductor Physics, Quantum Electronics and Optoelectronics*, 2003, **6**, 105-108.
12. L. Bjornstrom and M. Sjoberg, *Mol Endocrinol*, 2005, **19**, 833-842.
13. J. M. Hall, J. F. Couse and K. S. Korach, *J Biol Chem*, 2001, **276**, 36869-36872.
14. S. Jain, G. Spandana, A. K. Agrawal, V. Kushwah and K. Thanki, *Molecular pharmaceuticals*, 2015, **12**, 3871-3884.
15. S. R. Datir, M. Das, R. P. Singh and S. Jain, *Bioconjug Chem*, 2012, **23**, 2201-2213.
16. S. Jain, V. S. Thakare, M. Das, C. Godugu, A. K. Jain, R. Mathur, K. Chuttani and A. K. Mishra, *Chem Res Toxicol*, 2011, **24**, 2028-2039.
17. D. Ravelli, D. Merli, E. Quartarone, A. Profumo, P. Mustarelli and M. Fagnoni, *RSC Advances*, 2013, **3**, 13569-13582.
18. M. S. Levy, P. Lotfian, R. O'Kennedy, M. Y. Lo-Yim and P. A. Shamlou, *Nucleic Acids Res*, 2000, **28**, E57.
19. S. Jain, D. Kumar, N. K. Swarnakar and K. Thanki, *Biomaterials*, 2012, **33**, 6758-6768.
20. R. Singh, D. Pantarotto, D. McCarthy, O. Chaloin, J. Hoebeke, C. D. Partidos, J. P. Briand, M. Prato, A. Bianco and K. Kostarelos, *J Am Chem Soc*, 2005, **127**, 4388-4396.
21. S. M. Bachilo, M. S. Strano, C. Kittrell, R. H. Hauge, R. E. Smalley and R. B. Weisman, *Science*, 2002, **298**, 2361-2366.
22. G. Jia, H. Wang, L. Yan, X. Wang, R. Pei, T. Yan, Y. Zhao and X. Guo, *Environ Sci Technol*, 2005, **39**, 1378-1383.
23. B. Gigliotti, B. Sakizzie, D. S. Bethune, R. M. Shelby and J. N. Cha, *Nano letters*, 2006, **6**, 159-164.
24. J.-W. Shen, T. Tang, X.-H. Wei, W. Zheng, T.-Y. Sun, Z. Zhang, L. Liang and Q. Wang, *RSC Advances*, 2015, **5**, 56896-56903.
25. K. Kunath, A. von Harpe, D. Fischer, H. Petersen, U. Bickel, K. Voigt and T. Kissel, *J Control Release*, 2003, **89**, 113-125.
26. J. H. Shannahan, J. M. Brown, R. Chen, P. C. Ke, X. Lai, S. Mitra and F. A. Witzmann, *Small*, 2013, **9**, 2171-2181.